Rotational Capacity of Reinforced Concrete Beams

Ulfkjær, J. P.; Henriksen, M. S.; Brincker, Rune; Hansen, Lars Pilegaard; Heshe, Gert; Jensen, Jens Kristian Jehrbo

Published in:
Modern Design of Concrete Structures : Proceedings of Nordic Symposium, Aalborg University, May 3-5, 1995

Publication date:
1995

Document Version
Publisher's PDF, also known as Version of record

ROTATIONAL CAPACITY OF REINFORCED CONCRETE BEAMS

J. P. Ulfkjær, M. S. Henriksen, R. Brincker, L. P. Hansen, G. Heshe and J. K. Jehrbo
Aalborg University, Department of Building Technology and Structural Engineering,
Sohngaardsholmsvej 57, DK-9000 Aalborg, Denmark.

ABSTRACT

The European Structural Integrity Society-Technical Committee 9, has initiated a Round Robin on 'Scale Effects and Transitional Failure Phenomena of Reinforced Concrete Beams in Flexure'. In Denmark, Aalborg University is participating. The programme for Aalborg University involves an experimental programme where 120 reinforced concrete beams, 54 plain concrete beams and 324 concrete cylinders are tested. For the reinforced concrete beams four different parameters are varied. The slenderness is 6, 12 and 18, the beam depth is 100 mm, 200 mm and 400 mm giving nine different geometries, five reinforcement ratios between 0.14% and 1.57%, and the concrete has a compressive strength of approximately 60 MPa or 90 MPa. The beams are tested in three-point bending in a servo controlled materials testing system specially designed for the wide range of geometries. The casting of the beams is finished. The experiments are presently performed and will continue until the summer of 1995. At present only results for the beam type with the dimension 100 mm x 100 mm x 1200 mm of normal strength concrete for all the reinforcement ratios and for geometrically similar beams with the reinforcement ratio 1.57 % is available. The results are presented as non-dimensional ultimate bending moments and the rotational capacity. The results show that the ultimate non-dimensional bending moment is dependent on the reinforcement ratio, when the reinforcement ratio is small, and independent for larger reinforcement ratios and that the rotational capacity is dependent on the reinforcement ratio, especially increasing at low reinforcement ratios. For geometrically similar beams in different size scales the experiments show that the non-dimensional moment is decreasing with size and that the rotational capacity both increases and decreases with the size scale.

Key words: Rotational Capacity, Concrete Beams, Experiments, Size Effect.

1 INTRODUCTION

When designing concrete structures one of the most important tasks for the designer is to ensure that the theoretical fracture will occur as a ductile fracture. One of the measures of the ductility of a concrete structure is the rotational capacity. When designing concrete structures according to the theory of plasticity for one dimensional structures, it is very important that the plastic rotation in the critical cross-sections is lower than the rotational capacity. In most codes the rotational capacity is assumed only to be dependent on the non-dimensional size of the compression zone [1]. With the development of fracture mechanics and of fast numerical tools the it is evident that ductility of concrete structures is dependent on many other factors than just the strength and the stiffness of the steel and concrete used and the reinforcement arrangement. Instead it is realized that the type of fracture is also dependent on the size of the structure, the fracture energy of the concrete, etc. [2],[3],[4] and [5]. The influence of these parameters has so far not been fully investigated or understood. There is therefore a lack of knowledge of how the rotational capacity is dependent on several factors. CEB has therefore started task group 2.2 'Ductility Requirements for Structural Concrete - Reinforcement', [6]. Also the European Structural Integrity Society-Technical-Committee 9 (ESIS-TC9) on concrete, chaired by professor Alberto Carpinteri has initiated a Round Robin on 'Scale Effects and Transitional Failure Phenomena of Reinforced Concrete Beams in Flexure'. The programme involves both experimental and numerical contributions. At Aalborg University the experimental programme with four different parameters is started. The slenderness is 6, 12 and 18, and the beam depth is 100 mm, 200 mm or 400 mm giving nine different geometries, the reinforcement ratio is between 0.14% and 1.57% and the concrete has a compressive strength of approximately 60 MPa or 90 MPa.

2 EXPERIMENTS

2.1 Materials

Concrete

At present only beams of normal strength concrete have been tested. The same mix is used for all the beams. Since the cross section of the smallest beams is only 100 mm x 100 mm, the largest aggregate size is chosen as 8 mm. The mix of the concrete is shown in Table 1. The mechanical properties were determined using standard tests. The cylinder compressive strength and the modulus of elasticity for the concrete were determined on 100 mm x 200 mm cylinders. The bending tensile strength and the bending fracture energy was determined on beams with a span of 800 mm and a cross-section of 100 mm x 100 mm. The cylinders and the fracture energy beams were cured in water at 20°C until the moment of testing. Before testing a notch of half the beam depth was diamond saw cut in the beams. In the bending fracture energy tests the feedback signal consisted of contributions from the stroke and the crack opening displacement. The constitutive parameters for the concrete are summarized in table 2.

Table 1: Mix proportions of the concrete.

Contents	kg/m^3	l/m^3
Cement PC(A/HS/EA/G)	350	111
Water	159	159
Plastisizer	1.1	0.9
Gravel (4-8mm)	901	343
Sand (0-2 mm)	900	336
Air	0	50
Density	2311 kg/m^3	

Table 2: Mechanical properties of tested concrete (results from the first six castings). Units are [Mpa] for the strength and [J/m^2].

Cylinder compressive strength	Mean	59.4
	S.Dev	5.89
Cylinder splitting tensile strength	Mean	3.83
	S.Dev	0.73
Modulus of elasticity	Mean	36.344
	S.Dev	1854
Bending tensile strength	Mean	5.17
	S.Dev	0.22
Bending fracture energy	Mean	126.8
	S.Dev	30.04

Table 3. Constitutive characteristics for the reinforcement.

Steel type	Modulus of elasticity [MPa]	Yield Strength [MPa]	Yield Capacity [-]	Ultimate Strength [MPa]	Ultimate Strain [-]
ø4	1.65E5	609	0	609	1.41E-2
ø5	2.09E5	744	0	744	2.57E-2
ø10	2.24E5	663	2.28E-2	738	11.2E-2
ø20	2.65E5	774	1.13E-2	911	9.27E-2

Steel

Four different ribbed steel bar diameters were used. The constitutive parameters for the steel were determined by uniaxial tensile tests and are summarized in table 3. The yield capacity is the horizontal part of the stress-strain curve until hardening occurs. The ø4 and ø5 steel bars were cold deformed, and the yield capacity was very small.

2.2 Testing equipment

The beams were submitted to three-point bending in a specially designed servo-controlled material testing system. Due to the many different geometries a flexible test setup was built. A photo of the test setup for the second largest beam type (with a depth of 400 mm, a width of 200 mm and a span of 7200 mm) is shown in figure 1. When changing the beam size the two columns supporting the beam are moved horizontally. At both supports horizontal displacement and rotations were allowed and at one support rotation around the beam axis was also allowed. At the load point rotations were allowed around two axes. This should minimize the influence of axial normal forces and torsion. At both end a stop was placed at the top of the beam to prevent the beam from sliding off the supports.

The stroke was measured using the build in LVDT (Linear Variable Differential Transformer) with a base of 100 mm. The vertical displacements were measured at eight points. The base of these LVDTs were 4 mm, 10 mm, 20 mm, 40 mm or 100 mm depending on the beam size and the position of each LVDT. The horizontal displacements beam were measured at both beam ends using two LVDTs with a base of 10 mm or 20 mm. The beam rotations were measured using a number (at least equal to half the slenderness ratio plus one) of specially designed measuring

frames. The frames were attached to the beams at three points and with three LVDTs attached to each frame. The LVDTs were thus measuring the displacement between two frames at three points. By assuming that plane sections remain plane it is possible to calculate the mean strain field in each measuring field. The base of the LVDTs attached to the measuring frames were 2.6 mm, 10.0 mm, 20.0 mm or 40.0 mm depending on the position of the LVDT and the size of the beam.

All signals and the time t (for the beams with slenderness ratio 18 there were 40 signals) were recorded using a data logger. The signals were recorded every three seconds.

2.3 Testing Procedure

Especially for the lower reinforcement ratios it is necessary to take the formation of crack growth in the tensile side of the beam into consideration when controlling the piston displacement. The tests were therefore controlled by a signal that included contributions from both the piston displacement and from an extra set of frames placed around the mid-section. The distance between the measuring frames was twice the beam depth in order to avoid the main crack to be beyond the measuring distance. At the bottom of one measuring frame an LVDT was attached measuring the distance between the two frames. The signal measured by this LVDT is called the crack opening displacement (COD), though the signal includes elastic contributions. The feedback signal δ was created by analog addition of the signals:

$$\delta = \alpha\delta_{stroke} + \beta\delta_{COD} \tag{1}$$

where δ_{stroke} is the signal from the built in LVDT and δ_{COD} is the signal from the COD. α and β are weight factors dependent on the beam size and the reinforcement ratio. The reference signal, a linear ramp, was generated from an AT PC. The loading rate was chosen so the crack load would be reached after 5-15 min. At later stages the rate was increased, and a typical experiment would take about 45 min. For some beams a deformation of more than 100 mm stroke was required. An unloading was therefore performed, steel plates were inserted between the beam and the piston, and a reloading was then performed. This procedure was repeated until fracture. Experiments with repeated loading could last up to several hours.

3 FRACTURE PARAMETER RESULTS

Different fracture parameter results were determined from the tests. A typical load-displacement curve is seen in figure 2 for the beam with span=4800 mm, depth=400 mm and width = 200 mm reinforced with 4 ø 20 mm giving a reinforcement ratio of 1.57 %. From the knowledge of the meassured changes in distance between two measuring frames in three points and by assuming that plane cross-sections remain plane the mean curvature of each measuring field was easily calculated. The displacement field along the beam axis is shown in figure 3, for the load points marked with an asterisk in figure 2. For the same loading points the distribution of the curvature along the beam axis is shown in figure 4. It is clearly seen that the rotations are localized in the centre field.

3.1 Non-Dimensional Ultimate Moment

Two different non-dimensional ultimate moments μ_1 and μ_2 were calculated. μ_1 is determined as the maximum moment divided by the section modulus W and the compressive strength (corresponding to the Bernoulli beam theory)

$$\mu_l = \frac{M}{W\sigma_c} = \frac{3PL}{2bh^2\sigma_c} \tag{2}$$

where P is the load, L is the span, b is the width and h is the depth, whereas μ_2 is the maximum bending moment divided by the ultimate yielding bending moment M_y (corresponding to the plasticity theory)

$$\mu_2 = \frac{M}{M_y} = \frac{PL}{4A_s\sigma_u h_{ef}} \tag{3}$$

where h_{ef} is the effective beam depth (the distance from the center of the reinforcement to the top of the beam), A_s is the cross sectional area of the reinforcement and σ_u is the tensile strength of the steel. μ_l is used to show the influence of the size, whereas μ_2 shows the influence of changing the reinforcement ratio. In the following figures 2-8 the mean values of three experiment are shown together with the minimum and maximum values marked with a vertical line. In figure 5 the μ_2 is shown for the beam type with span 1200 mm, depth 100 mm and thickness 100 mm. It is seen that μ_2 is decreasing for increasing reinforcement ratios. For larger reinforcement ratios μ_2 is almost constant, this is due to the fact that the tensile strength has an influence for small

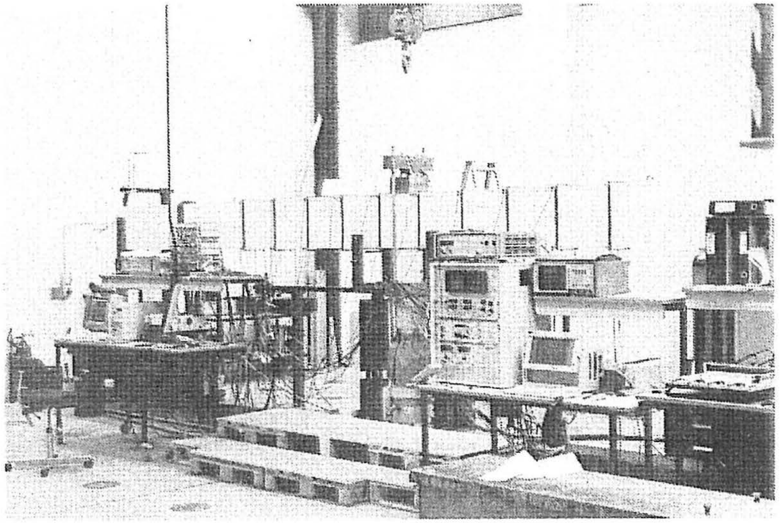

Figure 1. Photo of the test set-up for beams with the size: span 4800 mm; depth 400 mm; width 200 mm.

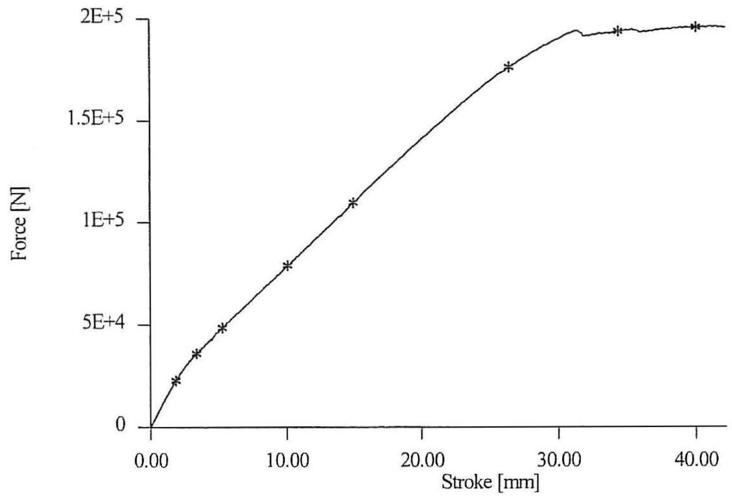

Figure 2. Typical load displacement curve for the beam size: apan 4800mm; depth 400mm; width 200 mm;

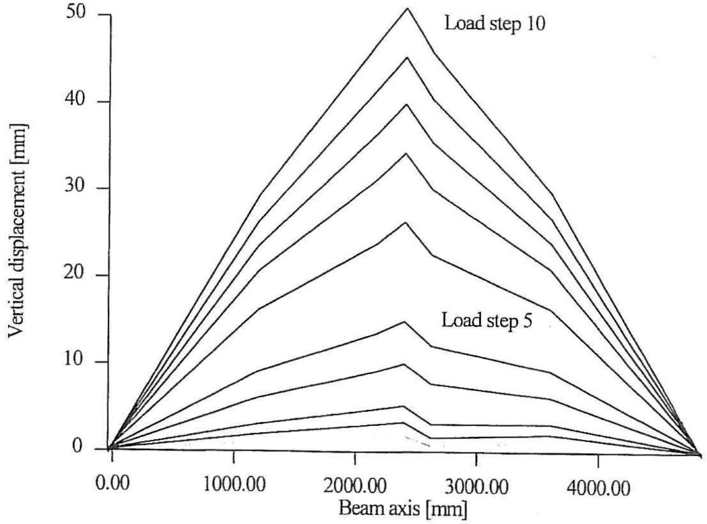

Figure 3. Vertical displacement distribution along the beam axis for the experiment in figure 2. The load levels are marked in figure 2 with asterisks.

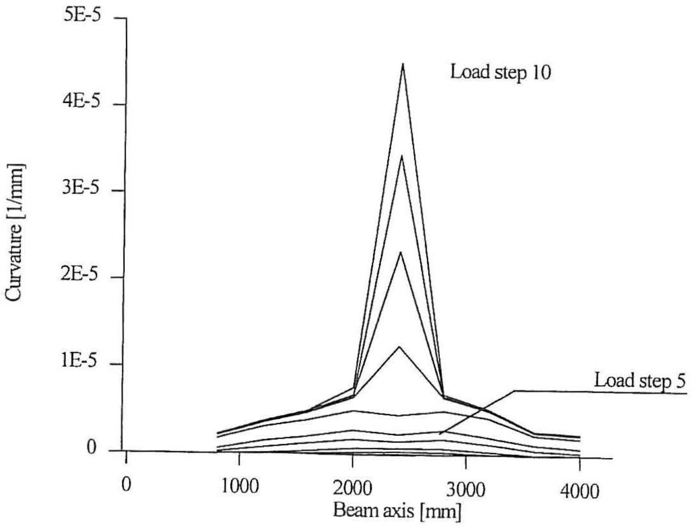

Figure 4. Curvature distribution along the beam axis for the experiment in figure 2. The load levels are marked in figure 2 with asterisks.

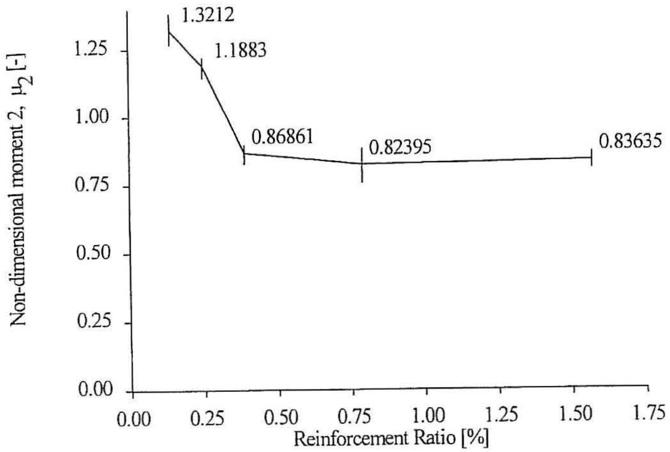

Figure 5. Non-dimensional moment as a function of the degree of reinforcement for the beam size: span 1200 mm; depth 100 mm; width 100 mm.

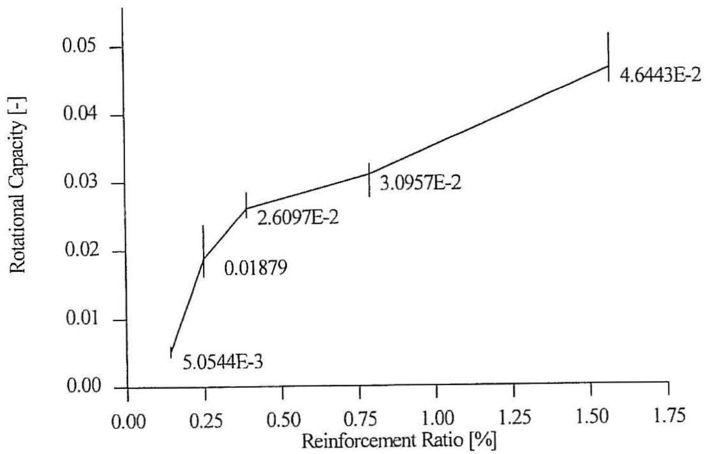

Figure 6. The rotational capacity as a function of the degree of reinforcement for the beam size: span 1200 mm; depth 100 mm; width 100 mm.

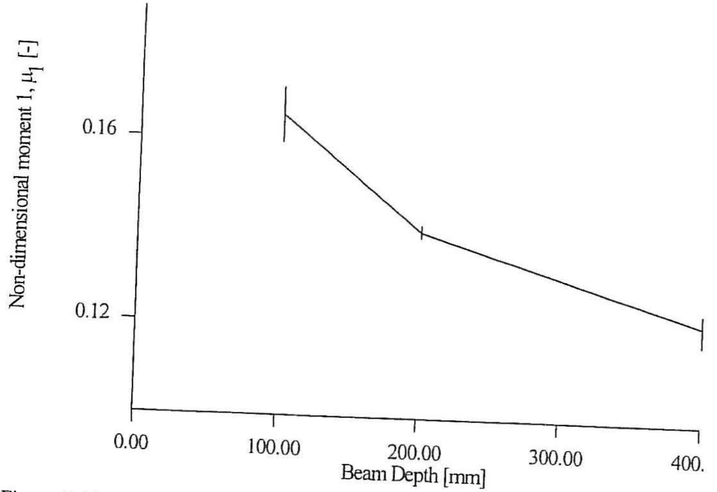

Figure 7. Non-dimensional moment as a function of the beam size for the degree of reinforcement 1.57 %.

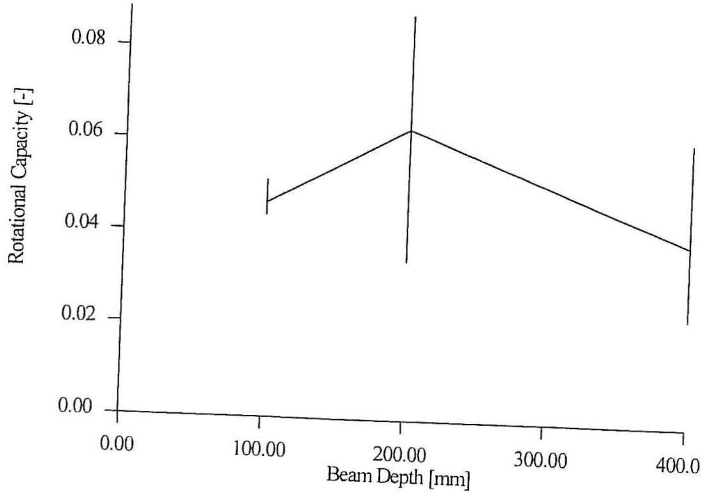

Figure 8. The rotational capacity as a function of the beam size for the reinforcement ratio 1.57% and slenderness 12.

reinforcement ratio. In figure 7 μ_l is shown as a function of the beam depth of geometrically similar beams (slenderness ratio equal to 12) with the reinforcement ratio 1.57 %. It is seen that μ_l is decreasing with the beam size. The decrease is about 25 % and is known as the size effect.

3.2 Rotational Capacity

The rotational capacity was calculated according to

$$\Theta_{pl} = \int_{0}^{L} \left(\kappa_{pl}^{*}(x) - \kappa_{el}^{*}(x) \right) dx \tag{4}$$

where κ_{el}^{*} is the elastic curvature at F^{*}, κ_{pl}^{*} is the total curvature at F^{*} and Θ_{pl} is the rotational capacity. With this definition the rotational capacity will be dependent on how F^{*} is chosen. Here F^{*} is chosen as the peak load even though a lot of plasticity is not taken into consideration. In figure 6 the rotational capacity is shown for a beam type with span 1200 mm, depth 100 mm and thickness 100 mm. It is seen that the rotational capacity is inceasing for inreasing reinforcement ratios and especially for the lower reinforcement ratios. In figure 8 the rotational capacity is shown as a function of the beam depth of geometrically similar beams (slenderness ratio equal to 12) for the reinforcement ratio 1.57 %. It is seen that the rotational capacity is almost independent of the beam size, however the scatter is very large making it difficult to make any conclusions.

4 CONCLUSION

A large test programme is performed in connection with the ESIS-TC9 round robin on Scale Effects and Transitional Failure Phenomena of Reinforced Concrete Beams in Flexure. In Aalborg University more than 120 beams are tested. The casting of the beams is finished. The experiments are presently performed and will continue until the summer of 1995. At present only results for the beam type with the dimension 100 mm by 100 mm by 1200 mm for all reinforcement ratios of normal strength concrete and results at different size scales for the reinforcement ratio 1.57 % are available. The results are presented as selected non-dimensional load displacement curves. Further, ultimate non-dimensional bending moments and the rotational capacity are calculated. The results show that the ultimate non-dimensional bending moment is dependent on the reinforcement ratio when the reinforcement ratio is small and independent for larger reinforcement ratios, and that the rotational capacity is dependent on the reinforcement ratio, especially increasing at low reinforcement ratios. For geometrically similar beams is seen that a size effect is present on the load carrying capacity. Due to the large scatter on the temporary results for the rotational capacity it is for the time being difficult to give any conclusions regarding the influence on size on the rotational capacity.

6 ACKNOWLEDGEMENTS

The financial support from the Danish Technical Research Council (STVF) is gratefully acknowledged.

7 REFERENCES

[1] Comite Euro-Internationl du Beton (CEB), "*CEB-FIP Model Code 1990 - First draft*", Bulletin D'Information N°196, pp. 3.39 - 3.40 (1990).

[2] Hillerborg, A." Fracture Mechanics Concepts Applied to Moment Capacity and Rotational Capacity of Reinforced Concrete Beams", *Engineering Fracture Mechanics*, Vol. 35, pp.233-240, 1990.

[3] Cederwall, K., Losberg, A. and Palm, G., "Armereda Betonbalkars Rotationskapasitet", *Journal of the Nordic Concrete Federation*, Vol 4, pp. 9-16, 1974. (In Swedish)

[4] Bigaj, A. and Walraven, J.C., "Size Effect on Rotational Capacity of Plastic Hinges in Reinforced Concrete Beams", CEB,Bulletin D'Information N°218, pp. 7-23 (1993).

[5] Bosco, C. and Carpinteri, Al., " Scale Effects and Transitional Phenomena of Failure in Reinforced Concrete Beams", *ESIS Technical Comitee 9 on Concrete*, Vienna, pp. 1- 12, 1992.

[6] Comite Euro-Internationl du Beton (CEB), "Ductility - Reinforcement ",CEB,Bulletin D'Information N°218, pp. 1 - 273 (1993).

SHEAR STRENGTH OF NON SHEAR REINFORCED CONCRETE BEAMS

Jin Ping Zhang
Department of Structural Engineering
Technical University of Denmark
Building 118,2800 Lyngby,Denmark

ABSTRACT

It has been observed that, in general, the shear failure of non shear reinforced concrete beams is featured by the formation of a critical diagonal crack. In this paper, a physical explanation is given for this fact under the hypothesis that the cracking of concrete introduces potential yield lines which may be more dangerous than the ones found by the usual plastic theory. The critical diagonal cracking load is a problem of fracture mechanics, while the ultimate load carrying capacity is found according to the plastic theory. The strength of cracked concrete is expressed by introducing a factor which reflects the reduction of sliding resistance of concrete due to cracking. Theoretical calculations are compared with the experimental results of reinforced concrete beams. Good agreement has been found.

Key Words: Shear Strength, Concrete Beams, Diagonal Cracks.

1. INTRODUCTION

Shear failure mechanism and shear strength of reinforced concrete beams have been the subject of research for many years[1][2].

Among the many attempts to solve the shear problem, the plastic theory for non shear reinforced concrete beams and slabs was developed in the 70's by works of Nielsen et al[3][4][5][6]. An effectiveness factor had to be introduced in order to get agreement with experimental results. It turned out that, besides the usual and easily understandable parameters, the effectiveness factor also contained the influence of the shear span ratio, the physical meaning of which has never really been understood.

Observations from experiments show that the shear failure of non shear reinforced concrete beams with a normal shear span ratio is governed by the formation of a critical diagonal crack. Since the sliding strength is reduced considerably by the cracking, this phenomenon suggests that the cracking of concrete introduces potential yield lines which are more dangerous than those predicted by the usual plastic theory.

Under this hypothesis, the load carrying capacity of reinforced concrete beams may be calculated by plastic theory with an effectiveness factor containing effects of only quite natural parameters such as the compressive strength of concrete, the reinforcement ratio and a size effect parameter. The influence of cracking is taken into account by a reduction factor.